PERGAMON

Available online at www.sciencedirect.com

SCIENCE DIRECT®

Automatica 39 (2003) 1597–1606

automatica

www.elsevier.com/locate/automatica

Brief Paper

Control of mixing by boundary feedback in 2D channel flow☆

Ole Morten Aamo[a,*], Miroslav Krstić[b], Thomas R. Bewley[b]

[a] *Department of Engineering Cybernetics, Norwegian University of Science and Technology, Trondheim, N-7491, Norway*

[b] *Department of Mechanical and Aerospace Engineering, University of California, San Diego, CA 92093-0411, USA*

Received 17 July 2001; received in revised form 24 March 2003; accepted 7 April 2003

Abstract

We address the problem of enhancing mixing by means of boundary feedback control in 2D channel flow. This is done by first designing feedback control strategies for the stabilization of the parabolic equilibrium flow, then applying this feedback with the sign of the input reversed. The result is enhanced instability of the parabolic equilibrium flow, which leads rapidly to highly complex flow patterns. Simulations of the deformation of dye blobs positioned in the flow indicate (qualitatively) that effective mixing is obtained for small control effort as compared with the nominal (uncontrolled) flow. A mixedness measure P_ε is constructed to quantify the mixing observed, and is shown to be significantly enhanced by the application of the destabilizing control feedback.

Keywords: Mixing control; Flow control; Partial differential equations; Boundary control; Lyapunov

1. Introduction

In many engineering applications, the mixing of two or more fluids is essential to obtaining good performance in some downstream process (a prime example is the mixing of air and fuel in combustion engines (Annaswamy & Ghoniem, 1995). As a consequence, mixing has been the focus of much research, but without reaching a unified theory, either for the generation of flows that mix well due to external forcing, or for the quantification of mixing in such flows. Approaches range from experimental design and testing to modern applications of dynamical systems theory. The latter was initiated by Aref (1984), who studied chaotic advection in the setting of an incompressible, inviscid fluid contained in a (2D) circular domain, and agitated by a point vortex (the blinking vortex flow). Ottino and coworkers studied a number of various flows, examining mixing properties based on dynamical systems techniques (Ottino, 1989). Later Rom-Kedar, Leonard, and Wiggins (1990) applied Melnikov's method and KAM (Kolmogorov–Arnold–Moser) theory to quantify transport in a flow governed by an oscillating vortex pair. An obvious shortcoming of this theory is the requirement that the flow must be periodic, as such methods rely on the existence of a Poincaré map for which some periodic orbit of the flow induces a hyperbolic fixed point. Another shortcoming is that they can only handle small perturbations from integrability, whereas effective mixing usually occurs for large perturbations. A third shortcoming is that traditional dynamical systems theory is concerned with asymptotic, or long-time, behavior, rather than quantifying rate processes which are of interest in mixing applications. In order to overcome some of these shortcomings, recent advances in dynamical systems theory have focused on finding coherent structures and invariant manifolds in experimental datasets, which are finite in time and generally aperiodic. This has led to the notions of finite-time hyperbolic trajectories with corresponding finite-time stable and unstable manifolds (Haller & Poje, 1998). The results include estimates for the transport of initial conditions across the boundaries of coherent structures. Another method for identifying regions in a flow that have similar finite-time statistical properties based on ergodic theory was developed by Mezić and Wiggins (1999). The relationship between the two methods mentioned, focusing on geometrical and statistical

☆ This paper was not presented at any IFAC meeting. This paper was recommended for publication in revised form by Associate Editor Jessy W. Grizzle under the direction of Editor Hassan Khalil. This work was supported by NFR, ONR, AFOSR, and NSF. A more detailed report of the work can be obtained from the corresponding author, O.M. Aamo.

* Corresponding author. Tel.: +47-73594386.

E-mail addresses: aamo@itk.ntnu.no (O.M. Aamo), krstic@ucsd.edu (M. Krstić), bewley@ucsd.edu (T. Bewley).

0005-1098/03/$ - see front matter © 2003 Elsevier Ltd. All rights reserved.
doi:10.1016/S0005-1098(03)00140-7

properties of particle motion, respectively, was examined by Poje, Haller, and Mezić (1999). As these developments have partly been motivated by applications in geophysical flows, they are diagnostic in nature and lend little help to the problem of *generating* a fluid flow that mixes well. The problem of generating effective mixing in a fluid flow is usually approached by trial and error using various "brute force" open-loop controls, such as mechanical stirring or jet injection. However, D'Alessandro, Dahleh, and Mezić (1999) used control systems theory to rigorously derive the mixing protocol that maximizes entropy among all the possible periodic sequences composed of two shear flows orthogonal to each other.

In this paper, we propose using active feedback control in order to enhance existing instability mechanisms in a 2D model of plane channel flow. The fluid is considered incompressible and Newtonian (constant viscosity). Our hypothesis is that effective mixing may be obtained by enhancing the instability of the parabolic profile of the Poiseuille flow using boundary control. Furthermore, it is expected that by applying boundary control intelligently in a feedback loop, mixing will be considerably enhanced with relatively small control effort. We focus on decentralized control laws and design two different controllers based on Lyapunov stability analysis. We proceed by comparing the performance of the control laws in order to select a controller that has a significant stabilizing effect on the 2D flow. Finally, we switch the sign of the feedback gain to obtain a destabilizing control algorithm. It is recognized that channel flow instability mechanisms are inherently 3D. Efforts that study the stabilization problem only in 2D are thus inconclusive about physical flows, for which 3D effects are quite significant. (However, the " model problem" of 2D channel flow stabilization is a useful testbed for techniques that can eventually be extended to 3D flows.) When studying the problem of destabilization, however, the situation is markedly different. In this case, studying the 2D problem, rather than being inconclusive about physical flows, is indeed conservative: the neglected 3D instability mechanisms may be expected to substantially increase the rate of mixing beyond that seen in the 2D model presented here. Thus, the study of 2D flow destabilization has important consequences for physical, 3D flows. The controller developed by Balogh, Liu, and Krstić (2001) form the motivation for the decentralized control approach performed in the present paper. As noted in Balogh et al. (2001) and Bewley (2001), fully decentralized controllers have an implementational advantage in that they can be embedded into MEMS (Micro-Electro-Mechanical-Systems) hardware, minimizing the communication requirements of centralized computations and facilitating scaling to massive arrays of sensors and actuators.

The paper carries two general messages, which are beyond flow control. First, unlike in many control problems, the plant being controlled is of very high dimension and is nonlinear. In such a situation one would expect to necessitate an extremely complex control algorithm (possibly some form of a finite-horizon optimal control). Such a controller would not be implementable as it would require prohibitive computation and extensive wiring between the sensors, the actuators, and the computer(s). It is therefore remarkable that the control proposed, and demonstrated numerically to be very effective, is a static output feedback (i.e., proportional), decentralized, controller. Second, unlike most control problems, the problem of mixing considered here does not require stabilization but destabilization. We design such a controller, which does not drive the states (or the control inputs) unbounded but it does locally destabilize the system, leading to bounded unsteadiness in the system, and, indirectly, to enhanced mixing in the fluid.

The paper is organized as follows: in Section 2 we state the Navier–Stokes equation for incompressible flow, and derive the equation for the perturbation; in Section 3, we present the Lyapunov analysis for the design of boundary control laws; in Section 4, we present results from numerical simulations of the stabilizing and destabilizing cases; we offer some concluding remarks in Section 5.

2. Problem statement

The dimensionless Navier–Stokes equations for incompressible flow between two walls are given by

$$\begin{aligned} &\mathbf{W}_t - \tfrac{1}{R}\Delta\mathbf{W} + (\mathbf{W}\cdot\nabla)\mathbf{W} + \nabla P = 0, \\ &div\,\mathbf{W} = 0 \end{aligned} \tag{1}$$

for $0 < x < L$, $-1 < y < 1$, and $t > 0$, where $\mathbf{W} = \mathbf{W}(x,y,t) = (U(x,y,t), V(x,y,t))^{\mathrm{T}}$ is the velocity at location (x,y) and time t, $P = P(x,y,t)$ is the pressure at location (x,y) and time t, and R is the Reynolds number. Eq. (1) has a steady solution, or fixed point $(\bar{U},\bar{V})$, given as

$$\bar{U}(y) = 1 - y^2, \tag{2}$$

$$\bar{V} = 0 \tag{3}$$

with pressure $\bar{P} = -2x/R$. The geometry of the problem is illustrated in Fig. 1, along with the parabolic equilibrium profile. The stability characteristics of $(\bar{U},\bar{V})$ vary with the Reynolds number. For $R < 5772$, $(\bar{U},\bar{V})$ is linearly stable (see, for instance, Panton (1996)), that is, infinitesimal perturbations from the parabolic profile will be damped out. For

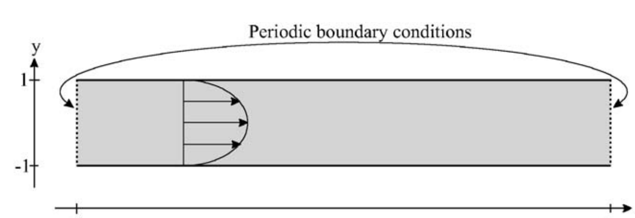

Fig. 1. Geometry of the flow problem.

$R > 5772$, $(\bar{U}, \bar{V})$ is unstable. Our main objective in this paper is to enhance mixing in the channel flow. Towards that end, we first design control laws that are analytically proved to enhance stability for small Reynolds numbers, and show by simulations that they stabilize $(\bar{U}, \bar{V})$ for large Reynolds numbers. Then, we reverse the control gains to destabilize the flow and thereby enhance mixing.

Defining the error $\mathbf{w} = (u, v) = (U - \bar{U}, V)$, and defining $p = P - \bar{P}$, we get the following set of equations for the error:

$$\begin{aligned} u_t &= \frac{1}{R}(u_{xx} + u_{yy}) - uu_x - \bar{U}u_x - vu_y - v\bar{U}' - p_x, \\ v_t &= \frac{1}{R}(v_{xx} + v_{yy}) - uv_x - \bar{U}v_x - vv_y - p_y, \\ u_x &+ v_y = 0 \end{aligned} \tag{4}$$

for $0 < x < L$, $-1 < y < 1$, and $t > 0$, with initial conditions $u(x, y, 0) = u_0(x, y)$, $v(x, y, 0) = v_0(x, y)$. We assume periodic boundary conditions in the streamwise direction, that is, we equate the quantities $\mathbf{w}$ and p at $x = 0$ and $x = L$. The question of boundary conditions on the walls, $y = \pm 1$, is our control design problem, and is the focus of the next section.

3. Boundary control design

Boundary control laws for stabilization are sought such that a suitable measure of the perturbation (u, v), which we will call the perturbation energy of the system, decays as a function of time. This is a standard Lyapunov-based approach, in which the Lyapunov function is chosen as

$$E(\mathbf{w}) = \|\mathbf{w}\|_{L_2}^2 = \int_{-1}^{1}\int_0^L (u^2 + v^2)\,\mathrm{d}x\,\mathrm{d}y. \tag{5}$$

The time derivative of $E(\mathbf{w})$ along the trajectories of (4) is

$$\dot{E}(\mathbf{w}) = 2\int_{-1}^{1}\int_0^L (uu_t + vv_t)\,\mathrm{d}x\,\mathrm{d}y. \tag{6}$$

Inserting (4) into (6), and integrating by parts, we obtain

$$\begin{aligned} \dot{E}(\mathbf{w}) = &-\frac{2}{R}\int_{-1}^{1}\int_0^L (u_x^2 + u_y^2 + v_x^2 + v_y^2)\,\mathrm{d}x\,\mathrm{d}y \\ &- 2\int_{-1}^{1}\int_0^L vu\bar{U}'\,\mathrm{d}x\,\mathrm{d}y \\ &+ \int_{-1}^{1}\int_0^L (u^2 + v^2 + 2p)(u_x + v_y)\,\mathrm{d}x\,\mathrm{d}y \\ &+ \int_0^L \left[\frac{2}{R}(u_y u + v_y v) - 2pv - (u^2 + v^2)v\right]_{y=-1}^{1}\mathrm{d}x. \end{aligned}$$

Incompressibility $(u_x + v_y = 0)$ now gives

$$\begin{aligned} \dot{E}(\mathbf{w}) = &-\frac{2}{R}\int_{-1}^{1}\int_0^L (u_x^2 + u_y^2 + v_x^2 + v_y^2)\,\mathrm{d}x\,\mathrm{d}y \\ &- 2\int_{-1}^{1}\int_0^L uv\bar{U}'\,\mathrm{d}x\,\mathrm{d}y \\ &+ \int_0^L \left[\frac{2}{R}(u_y u + v_y v) \right. \\ &\left. - 2pv - (u^2 + v^2)v\right]_{y=-1}^{1}\mathrm{d}x. \end{aligned} \tag{7}$$

Following Balogh et al. (2001, Lemma 6.2), we set

$$u(x, y, t) = u(x, -1, t) + \int_{-1}^{y} u_y(x, \gamma, t)\,\mathrm{d}\gamma,$$

so that

$$u^2(x, y, t) \leqslant 2u^2(x, -1, t) + 2\left(\int_{-1}^{y} u_y(x, \gamma, t)\,\mathrm{d}\gamma\right)^2.$$

By the Cauchy–Schwartz inequality,

$$\left(\int_{-1}^{y} 1u_y(x, \gamma, t)\,\mathrm{d}\gamma\right)^2 \leqslant (y + 1)\left(\int_{-1}^{y} u_y^2(x, \gamma, t)\,\mathrm{d}\gamma\right),$$

so we have that

$$u^2(x, y, t) \leqslant 2u^2(x, -1, t) + 2(y + 1)\int_{-1}^{1} u_y^2(x, y, t)\,\mathrm{d}y,$$

where we have set $y = 1$ in the integral. Therefore, we get

$$\begin{aligned} \int_{-1}^{1}\int_0^L u^2\,\mathrm{d}x\,\mathrm{d}y \leqslant{}& 4\int_0^L u^2(x, -1, t)\,\mathrm{d}x \\ &+ 4\int_{-1}^{1}\int_0^L u_y^2(x, y, t)\,\mathrm{d}x\,\mathrm{d}y. \end{aligned}$$

An analogous derivation for v_y now gives

$$\begin{aligned} &-\int_{-1}^{1}\int_0^L (u_y^2 + v_y^2)\,\mathrm{d}x\,\mathrm{d}y \\ &\quad \leqslant -\frac{E(\mathbf{w})}{4} + \int_0^L (u^2(x, -1, t) + v^2(x, -1, t))\,\mathrm{d}x. \end{aligned} \tag{8}$$

Inserting (8) into (7) we get

$$\begin{aligned} \dot{E}(\mathbf{w}) \leqslant &-\frac{1}{2R}E(\mathbf{w}) \\ &+ \frac{2}{R}\int_0^L (u^2(x, -1, t) + v^2(x, -1, t))\,\mathrm{d}x \\ &- \frac{2}{R}\int_{-1}^{1}\int_0^L (u_x^2 + v_x^2)\,\mathrm{d}x\,\mathrm{d}y \\ &- 2\int_{-1}^{1}\int_0^L uv\bar{U}'\,\mathrm{d}x\,\mathrm{d}y \\ &+ \int_0^L \left[\frac{2}{R}(u_y u + v_y v) - 2pv - (u^2 + v^2)v\right]_{y=-1}^{1}\mathrm{d}x. \end{aligned}$$

Since

$$-2\int_{-1}^{1}\int_{0}^{L} uv\bar{U}'\,\mathrm{d}x\,\mathrm{d}y \leqslant 2\int_{-1}^{1}\int_{0}^{L}(u^2+v^2)\,\mathrm{d}x\,\mathrm{d}y = 2E(\mathbf{w}),$$

we finally get

$$\dot{E}(\mathbf{w}) \leqslant -\frac{1}{2}\left(\frac{1}{R}-4\right)E(\mathbf{w}) + \frac{2}{R}\int_0^L (u^2(x,-1,t)+v^2(x,-1,t))\,\mathrm{d}x + \int_0^L \left[\frac{2}{R}(u_y u + v_y v) - 2pv - (u^2+v^2)v\right]_{y=-1}^{1}\mathrm{d}x. \tag{9}$$

Notice that for $R<\frac{1}{4}$, $E(\mathbf{w})$ decays exponentially with time even in the uncontrolled case ($u(x,\pm1,t)=v(x,\pm1,t)\equiv 0$). In other words, the fixed point $(\bar{U},\bar{V})$ is globally exponentially stable (in L_2) in this case, and the goal of applying boundary control is to enhance stability.

Wall-tangential control: The following boundary control was suggested in by Balogh et al. (2001):

$$u(x,-1,t)=k_u u_y(x,-1,t), \tag{10}$$

$$u(x,1,t)=-k_u u_y(x,1,t), \tag{11}$$

$$v(x,\pm1,t)=0. \tag{12}$$

Inserting (10)–(12) into (9) gives

$$\dot{E}(\mathbf{w}) \leqslant -\frac{1}{2}\left(\frac{1}{R}-4\right)E(\mathbf{w}) - \frac{2}{R}\left(\frac{1}{k_u}-1\right)\int_0^L u^2(x,-1,t)\,\mathrm{d}x. \tag{13}$$

Thus, for $R<\frac{1}{4}$ and $k_u\in[0,1]$, $E(\mathbf{w})$ decays exponentially with time.

Wall-normal control: Actuation normal to the wall is another strategy of active interest. Inequality (9) also suggests a control law structure for wall-normal control. Setting $u(x,-1,t)=u(x,1,t)=0$, v_y is zero at the wall, so we have

$$\dot{E}(\mathbf{w}) \leqslant -\frac{1}{2}\left(\frac{1}{R}-4\right)E(\mathbf{w}) + \frac{2}{R}\int_0^L v^2(x,-1,t)\,\mathrm{d}x - 2\int_0^L [2pv]_{y=-1}^{1}\,\mathrm{d}x - \int_0^L [v^3]_{y=-1}^{1}\,\mathrm{d}x. \tag{14}$$

Now, by imposing $v(x,-1,t)=v(x,1,t)$, the last term in (14) vanishes. Thus, we propose the following control law:

$$u(x,\pm1,t)=0, \tag{15}$$

$$v(x,\pm1,t)=k_v(p(x,1,t)-p(x,-1,t)). \tag{16}$$

Inserting (15)–(16) into (14) gives

$$\dot{E}(\mathbf{w}) \leqslant -\frac{1}{2}\left(\frac{1}{R}-4\right)E(\mathbf{w}) - 2\left(\frac{1}{k_v}-\frac{1}{R}\right)\int_0^L v^2(x,-1,t)\,\mathrm{d}x. \tag{17}$$

Thus, for $R<\frac{1}{4}$ and $k_v\in[0,R]$, $E(\mathbf{w})$ decays exponentially with time. Furthermore, note that (16) ensures that the net mass flux through the walls be zero.

Implementation: In order to implement the above controllers we have to express them in terms of the actual flow variables, U, V and P. For the wall-tangential case, we get:

$$U(x,-1,t)=k_u(U_y(x,-1,t)-\bar{U}'(-1)), \tag{18}$$

$$U(x,1,t)=-k_u(U_y(x,1,t)-\bar{U}'(1)), \tag{19}$$

$$V(x,\pm1,t)=0 \tag{20}$$

and for the wall-normal case we get

$$U(x,\pm1,t)=0, \tag{21}$$

$$V(x,\pm1,t)=k_v(P(x,1,t)-P(x,-1,t)). \tag{22}$$

It is interesting to notice that the wall-normal control law is independent of the physical parameters of the flow. This is an important property, since the physical parameters of any real flow are subject to inaccuracy. In contrast, $\bar{U}'(x,\pm1,t)$ must be known for wall-tangential control. It is also worth noting that all the above control laws are of the Jurdjevic–Quinn (Jurdjevic & Quinn, 1978) type (with respect to the Lyapunov function $E(\mathbf{w})$). This endows these control laws with inverse optimality with respect to a meaningful cost functional (which is in these cases complicated to write).

4. Numerical demonstration

The main results of this section are that (1) the stabilizing control law stabilizes the 2D unsteady flow model for high values of Reynolds number, (2) the destabilizing control law achieves excellent mixing in the 2D flow model using small amounts of control effort. The reader is reminded of the comments made in the introduction about the conservative nature of the present 2D mixing results in light of the destabilizing 3D effects present in real channel flows at high values of the Reynolds number.

4.1. The computational scheme

The simulations are performed using a hybrid Fourier pseudospectral-finite difference discretization and the fractional step technique based on a hybrid Runge–Kutta/Crank–Nicolson time discretization using the numerical method of Bewley and Moin (1999). This method is particularly well suited even for the cases with wall-normal actuation

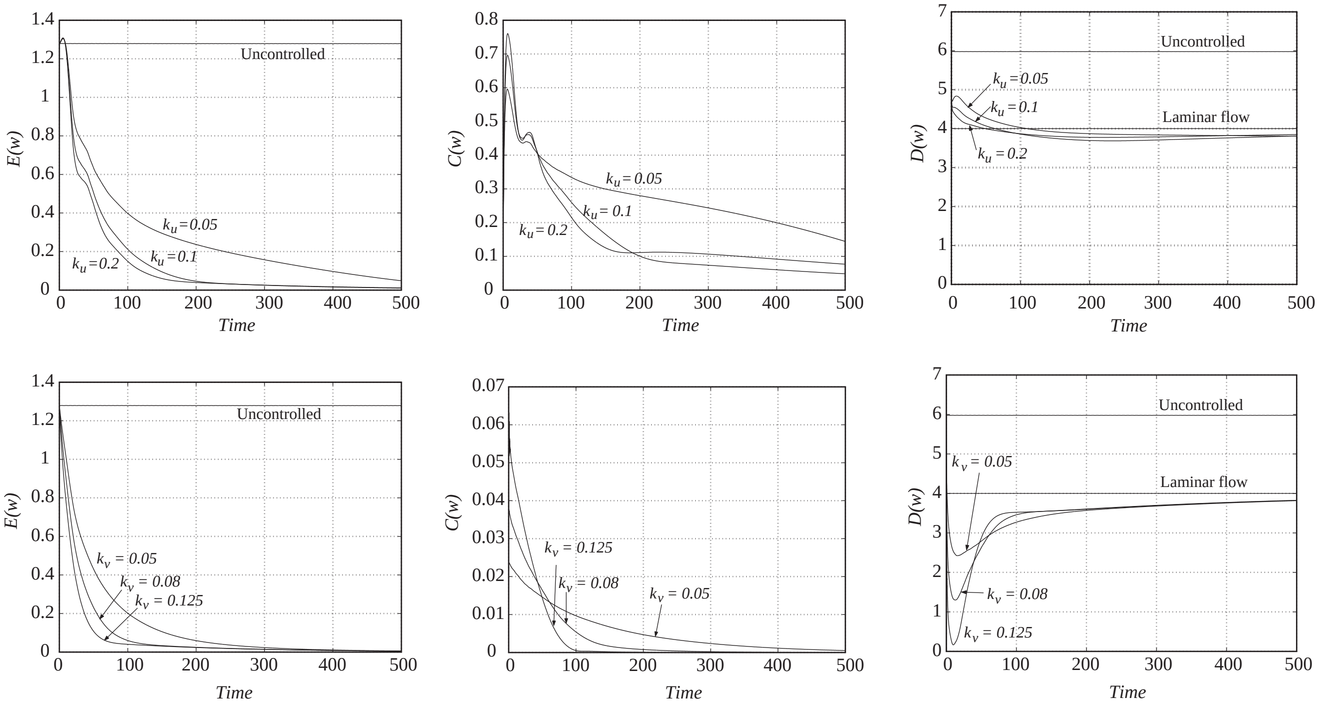

Fig. 2. Energy $E(\mathbf{w})$ (left), control effort $C(\mathbf{w})$ (middle), and drag $D(\mathbf{w})$ (right), as functions of time for wall-tangential actuation (upper row) and wall-normal actuation (lower row).

because of its implicit treatment of the wall-normal convective terms. The wall-parallel direction is discretized using 128 Fourier-modes, while the wall-normal direction is discretized using energy-conserving central finite differences on a stretched staggered grid with 100 gridpoints. The gridpoints have hyperbolic tangent distribution in the wall-normal direction in order to adequately resolve the high-shear regions near the walls. A fixed flow-rate formulation is used, rather than fixed average pressure gradient, since observations suggest that the approach to equilibrium is faster in this case (Jiménez, 1990). The difference between the two formulations is discussed briefly by Rozhdestvensky and Simakin (1984). The time step is in the range 0.05–0.07 for all simulations.

4.2. Stabilization

The theoretical results of Section 3 are only valid for Reynolds numbers less than $\frac{1}{4}$, for which the parabolic equilibrium profile is globally exponentially stable in the uncontrolled case. Thus, the analysis only tells us that the proposed control laws maintain stability, and not neccessarily enhance it. In fact, for wall-normal control, simulations at $R=0.1$ show that for $k_v=0.1$, $E(\mathbf{w})$ converges more slowly to 0 than in the uncontrolled case, whereas for $k_v=-0.1$, stability is enhanced. Although this result was unexpected, it does not contradict the theoretical results. Being valid for small Reynolds numbers only, the theoretical results are of limited practical value. However, they do suggest controller structures worth testing on flows having higher Reynolds numbers. Balogh et al. (2001) presented results from numerical simulations with wall-tangential control that show stabilization of channel flow at $R=15\,000$. Here, we do a comparison of the performance of the two control laws for flows at $R=7500$ and $L=4\pi$.

In addition to reporting the time evolution of the energy, $E(\mathbf{w})$, we also consider the (instantaneous) control effort and drag force as measures of performance. The control effort is defined as

$$C(\mathbf{w})=\sqrt{\int_0^L (|\mathbf{w}(x,-1,t)|^2+|\mathbf{w}(x,1,t)|^2)\,\mathrm{d}x} \tag{23}$$

and the drag force as

$$D(\mathbf{w})=\frac{1}{L}\int_0^L\left(\frac{\partial U}{\partial y}(x,-1,t)-\frac{\partial U}{\partial y}(x,1,t)\right)\mathrm{d}x. \tag{24}$$

Notice that (24) is really the mean wall shear, which is related to the drag force by the factor $1/\mu L$. For selected time instants, vorticity maps are also provided. The vorticity, ω, is defined using the actual flow variables (rather than the perturbation variables) as

$$\omega(x,y,t)=\frac{\partial V}{\partial x}(x,y,t)-\frac{\partial U}{\partial y}(x,y,t). \tag{25}$$

A total of six simulations are performed: wall-tangential control with $k_u\in[0.05,0.1,0.2]$, and; wall-normal control with $k_v\in[-0.125,-0.08,-0.05]$. As already mentioned, the parabolic equilibrium profile is unstable for $R=7500$,

Fig. 3. Vorticity map for the fully established 2D channel flow (uncontrolled).

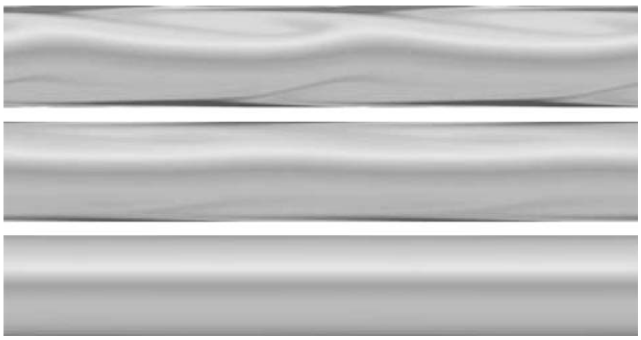

Fig. 4. Vorticity maps for wall-normal actuation at $t = 30$ (top figure), $t = 60$, and $t = 120$ (bottom figure). The feedback gain is $k_v = -0.125$.

so infinitesimal disturbances will grow, but the flow eventually reaches a statistically steady state, which we call *fully established flow*. For all simulations, the fully established flow, for which $E(\mathbf{w}) \approx 1.3$, is chosen as the initial data. Fig. 3 shows a vorticity map for the fully established (uncontrolled) flow. It is similar to vorticity maps presented in (Jiménez, 1990), and clearly shows the ejection of vorticity from the walls into the core of the channel as described in (Jiménez, 1990).

Fig. 2 compares wall-tangential and wall-normal control. It is clear that stabilization is obtained for both controllers in terms of the energy $E(\mathbf{w})$. Fig. 2 shows that $E(\mathbf{w})$ decays faster for wall-normal control, and at much less control effort (notice the different scales for $C(\mathbf{w})$ for the two cases in Fig. 2). The ratio of the peak kinetic energy of the control flow (wall normal), versus the perturbation kinetic energy in the uncontrolled case (drained out by the control), $C(\mathbf{w})^2/E(\mathbf{w})$, is less than 0.25%. Also, reduction of drag is more efficient in the wall-normal control case.[1]

Fig. 4 shows vorticity maps at three different time instances for wall-normal control with $k_v = -0.125$. The removal of vortical structures is evident already at $t = 30$ (top graph), and at $t = 120$ (bottom graph) the flow is nearly uniform. Fig. 5 shows the pressure field immediately after onset of wall-normal control ($k_v = -0.125$). Regions of low pressure coincide with regions of circulation cells, as the

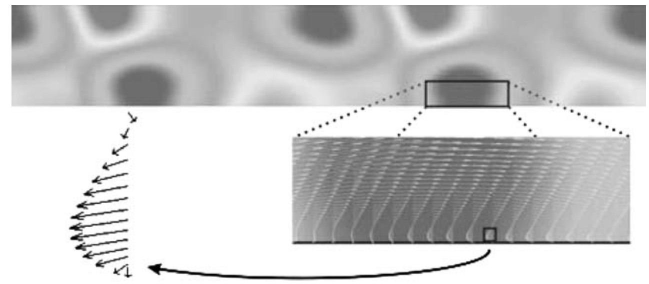

Fig. 5. Pressure (perturbation only, i.e. p) immediately after onset of wall-normal actuation. Zoom shows velocity vectors in a region with low pressure.

velocity vectors in the intermediate zoom show. In the most detailed zoom, we see that the controller applies suction in this region.

4.3. Mixing

Mixing is commonly induced by means of open-loop methods such as mechanical stirring or jet injection. These methods may use excessive amounts of energy, which in certain cases is undesirable. Thus, we propose using active feedback control in order to exploit the natural tendency in the flow to mix. To the authors' knowledge, this is the first attempt to induce mixing by means of feedback, as the mixing protocols thus far have been open loop controls. It was observed by Hammond, Bewley, and Moin (1998) that some heuristic control strategies enhance turbulence, although this observation was not made in the context of mixing but in the context of drag mitigation.

The results of the previous section show that the control law (15)–(16) has a significant stabilizing influence on the 2D channel flow. In this section, we explore the behaviour of the flow when k_v is chosen such that this feedback destabilizes the flow rather than stabilizes it. The conjecture is that the flow will develop a complicated pattern in which mixing will occur. 2D simulations are performed at $R = 6000$, for which the parabolic equilibrium profile is unstable. The vorticity map for the fully established flow (uncontrolled) at this Reynolds number is shown in the topmost graph in Fig. 6. This is the initial data for the simulations. Some mixing might be expected in this flow, as it periodically ejects vorticity into the core of the channel. Our objective, however, is to enhance the mixing process by boundary control, which we impose by setting $k_v = 0.1$ in (16). The vorticity maps in Fig. 6 suggest that the flow pattern becomes considerably more complicated as a result of the control. The left graph in Fig. 7 show the perturbation energy, $E(\mathbf{w})$, as a function of time, which increases by a factor of 5. It is interesting to notice that the control leading to such an agitated flow is small (see middle graph in Fig. 7). The maximum value of the control flow kinetic energy is less than 0.7% of the perturbation kinetic energy of the uncontrolled flow, and only about 0.1% of the fully developed, mixed (controlled)

[1] It is interesting to note (see Fig. 2) that, when the control is applied to the 2D flow, a transient ensues in which the drag dips below the laminar level and then asymptotes towards the laminar state. This transient, however, is dependent on the initial flow state being that of the fully established 2D flow, which has a drag which is significantly higher than laminar. Thus, this transient result does not disprove the conjecture stated by Bewley (2001).

flow! Fig. 8 shows the pressure field at $t = 150$, as well as velocity vectors in a region close to the wall. As for the stabilizing case, regions of low pressure coincide with regions of circulation cells, as the velocity vectors in the intermediate zoom show. In the most detailed zoom, we see that the controller applies blowing in this region. Next, we will quantify the mixing in a more rigorous way, and compare the controlled and uncontrolled cases.

A number of inherently different processes constitute what is called mixing. Ottino (1989) distinguishes between three sub-problems of mixing: (i) mixing of a single fluid (or similar fluids) governed by the stretching and folding of material elements; (ii) mixing governed by diffusion or chemical reactions; and (iii) mixing of different fluids governed by the breakup and coalescence of material elements. Of course, all processes may be present simultaneously. In the first sub-problem, the interfaces between the fluids are passive (Aref & Tryggvason, 1984), and the mixing may be determined by studying the movement of a passive tracer, or dye, in a homogeneous fluid flow. This is the problem we are interested in here.

The location of the dye as a function of time completely describes the mixing, but in a flow that mixes well, the length of the interface between the dye and the fluid increases exponentially with time. Thus, calculating the location of the dye for large times is not feasible within the restrictions of modest computer resources (Franjione & Ottino, 1987). We do, nevertheless, attempt this for small times, and supplement the results with less accurate, but computationally feasible, calculations for larger times. A particle-line method is used to track the dye interface. In short, this method represents the interface as a number of particles connected by straight lines. The positions of the particles are governed by the equation $dX/dt = (U(X,t), V(X,t))$, where X is a vector of particle positions. At the beginning of each time step, new particles are added such that at the end of the time step, a prescribed resolution, given in terms of the maximum length between neighboring particles, is maintained. The fact that we are working with a single fluid representing multiple miscible fluids, ensures that dye surfaces remain connected (Ottino, 1989). At $t = 50$, when the perturbation energy is about tripled in the controlled case (Fig. 7), 18 blobs are distributed along the centerline of the channel as shown in Fig. 9. They cover 25% of the total domain. Fig. 10 shows the configuration of dye in the controlled case for 5 time instances. The difference in complexity between the uncontrolled and controlled cases is clear (compare the lower graphs of Figs. 9 and 10), however, large regions are poorly mixed even at $t = 85$. The right graph in Fig. 7 shows the total length of the surface of the dye. The length appears to grow linearly with time in the uncontrolled case, whereas for the controlled case, it grows much faster, reaching values an order of magnitude larger than in the uncontrolled case. In order to approximate the dye distribution for large time, a fixed number of particles are uniformly distributed throughout the domain, distinguishing between particles placed on the inside (*black* particles) and on the outside (*white* particles) of regions occupied by dye. Fig. 11 shows the distribution of black particles at $t = 85$ (for comparison with Fig. 10), 100, 125 and 150. The particle distribution becomes increasingly uniform.

In order to quantify the mixing further, we ask the following question: given a box of size ε, what is the probability, P, of the fluid inside being *well mixed*? An appropriate choice of ε, and what is considered well mixed, are application specific parameters, and are usually given by requirements of some downstream process. In our case, the blobs

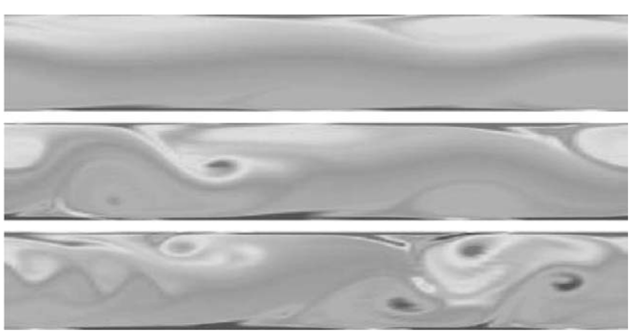

Fig. 6. Vorticity map for the fully established, uncontrolled, channel flow at $Re = 6000$ (top), and for the controlled case at $t = 50$ (middle) and $t = 80$ (bottom).

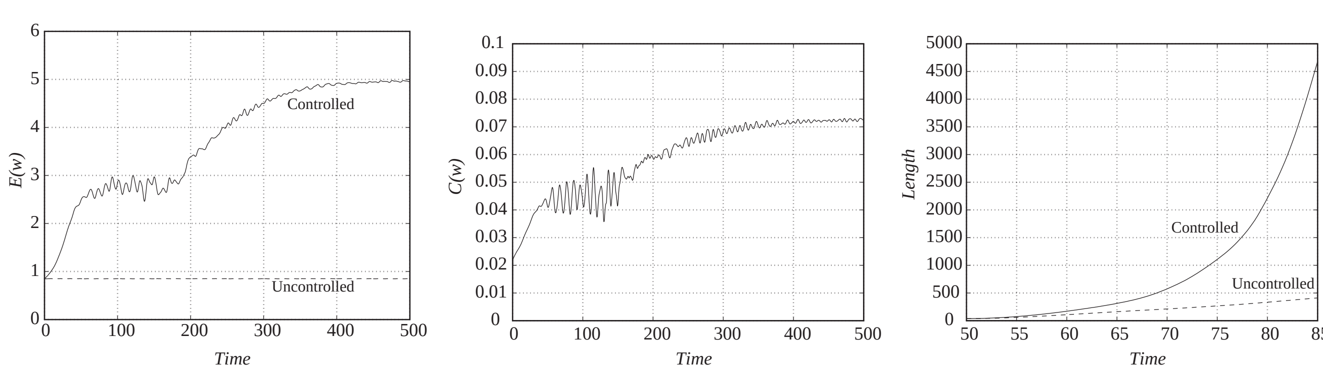

Fig. 7. Energy $E(\mathbf{w})$ (left), control effort $C(\mathbf{w})$ (middle), and dye surface length (right), as functions of time.

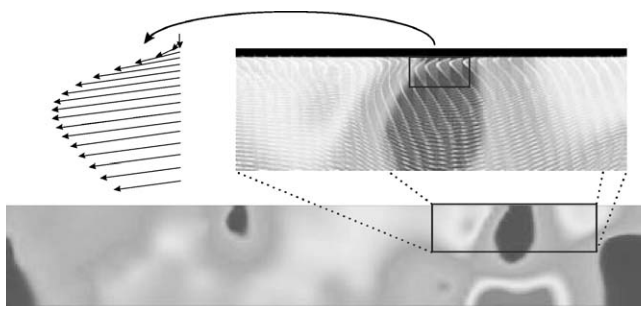

Fig. 8. Pressure (perturbation only, i.e. p) at $t = 150$. Zoom shows velocity vectors in a region with low pressure.

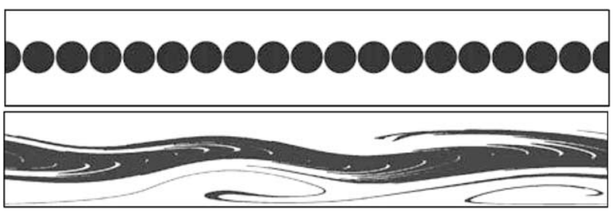

Fig. 9. Initial distribution of dye blobs (at $t = 50$), and dye distribution at $t = 85$ for uncontrolled flow.

initially cover 25% of the domain, so we will define *well mixed* to mean that the dye covers between 20% and 30% of the area of the box. The size ε of the boxes will be given in terms of pixels along one side of the box, so that the box covers ε^2 pixels out of a total of 2415×419 pixels for the entire domain. On this canvas, the box may be placed in $(419 - (\varepsilon - 1)) \times 2415$ different locations. The fraction of area covered by dye inside box i of size ε, is for small times calculated according to

$$c_\varepsilon^i = \frac{n_p}{\varepsilon^2}, \tag{26}$$

where n_p is the number of pixels covered by dye, and for large times according to

$$c_\varepsilon^i = \frac{n_b}{n_w + n_b}, \tag{27}$$

where n_b and n_w denote the number of black and white particles, respectively, contained in the box. P, which depends on ε, is calculated as follows:

$$P_\varepsilon = \frac{1}{n} \sum_{i=1}^{n} eval(0.2 < c_\varepsilon^i < 0.3), \tag{28}$$

where n is the total number of boxes. The expression in the summation evaluates to 1 when $0.2 < c_\varepsilon^i < 0.3$ and 0 otherwise. For small times $n = (419 - (\varepsilon - 1)) \times 2415$, whereas for large times n may be smaller as we choose to ignore boxes containing less than 25 particles. Figs. 12 and 13 show P_ε as a function of time for $\varepsilon \in [15, 30, 45, 60]$.

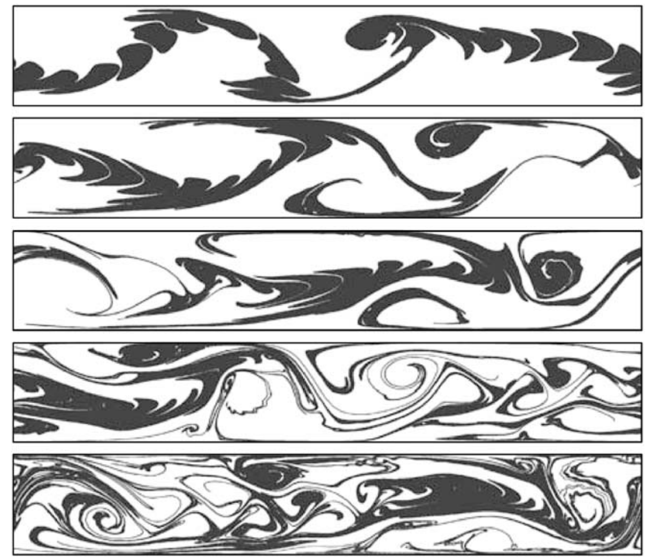

Fig. 10. Dye distribution for controlled flow at $t = 55$, 60, 65, 75 and 85 (from top towards bottom).

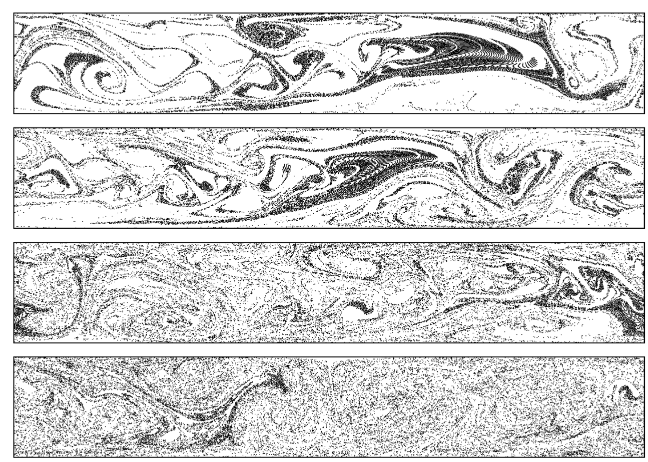

Fig. 11. Particle distribution for controlled flow at $t = 85$, 100, 125 and 150 (from top towards bottom).

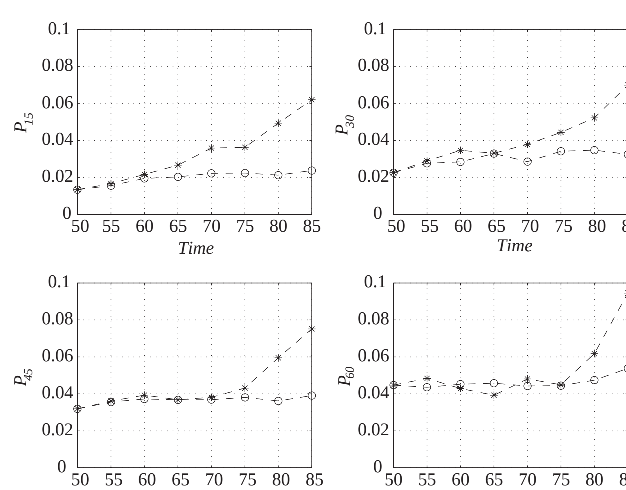

Fig. 12. Probability of well mixedness for the uncontrolled case (o) and controlled case (*).

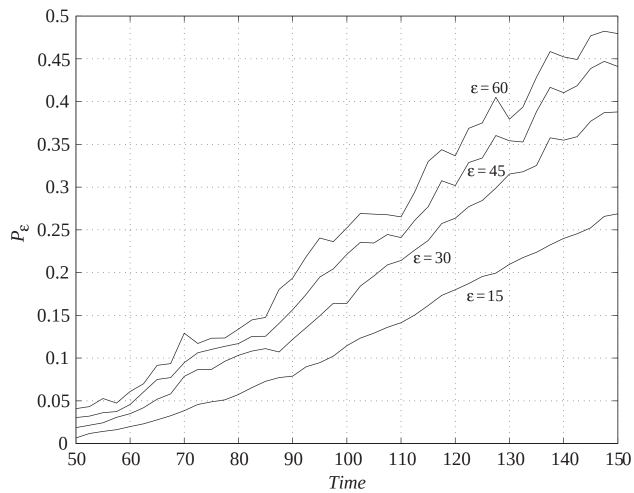

Fig. 13. Probability of well mixedness for the controlled case based on uniform particle distribution.

5. Conclusions

We have addressed the problem of imposing mixing by means of boundary feedback control in 2D channel flow. This is done by first designing control laws for the stabilization of the parabolic equilibrium profile, and then reversing the sign of the feedback gain in order to obtain destabilization. The result is a highly complex flow pattern, which leads to effective mixing.

Although the control design for the stabilization problem applies to small Reynolds numbers only, simulations show that the structure of the control laws predicted by the theory can be used to stabilize the 2D parabolic equilibrium profile for Reynolds number several orders of magnitude higher. We can not tell from the simulations whether the controllers render the equilibrium profile globally stable; however, it is clear that the fully established 2D flow, which is the most likely initial condition, is contained in the region of attraction. Another key point of the feedback laws presented, is the fact that they are completely decentralized. That is, control actuation at a location on the wall is simply a function of measurements at that same location, a fact that allows for decentralized computations and simple instrumentation. Simulations of the stabilization problem show that the performance obtained using wall-normal control is considerably better than that obtained using wall-tangential control. Also, the wall-normal control law has the important property that it is independent of the physical parameters of the flow. In contrast, the wall shear stress of the parabolic equilibrium profile must be known in order to implement the wall-tangential control.

Simulations using the wall-normal control law with the sign of the input reversed show that the flow pattern becomes considerably more complex than in the case of fully established uncontrolled flow. This suggests improved mixing, which is confirmed by studies of the behavior of dye blobs positioned in the flow. The length of the interface between dye and fluid appears to grow linearly with time in the uncontrolled case, but grows highly nonlinearly and reaches values approximately an order of magnitude larger in the controlled case. An alternative measure of performance, the probability of well mixedness, also indicates considerable improved mixing in the controlled case. The mixing is obtained by a small control effort, compared to the reference velocity of the flow. This is the main advantage of applying control intelligently in a feedback loop.

Acknowledgements

We thank Peter Blossey for providing the channel flow computer code used for the simulations, and for his helpful comments while adapting it to the two-dimensional boundary control problem. We also thank Andras Balogh for various discussions.

References

Annaswamy, A. M., & Ghoniem, A. F. (1995). Active control in combustion systems. *IEEE Control Systems*, *15*(6), 49–63.

Aref, H. (1984). Stirring by chaotic advection. *Journal of Fluid Mechanics*, *143*, 1–21.

Aref, H., & Tryggvason, G. (1984). Vortex dynamics of passive and active interfaces. *Physica D*, *12*, 59–70.

Balogh, A., Liu, W.-J., & Krstić, M. (2001). Stability enhancement by boundary control in 2D channel flow. *IEEE Transactions on Automatic Control*, *46*(11), 1696–1711.

Bewley, T. R. (2001). Flow control: New challenges for a new renaissance. *Progress in Aerospace Sciences*, *37*, 21–58.

Bewley, T. R., & Moin, P. (1999). Technical report TF-76, Stanford University.

D'Alessandro, D., Dahleh, M., & Mezić, I. (1999). Control of mixing in fluid flow: A maximum entropy approach. *IEEE Transactions on Automatic Control*, *44*(10), 1852–1863.

Franjione, J. G., & Ottino, J. M. (1987). Feasibility of numerical tracking of material lines and surfaces in chaotic flows. *Physics of Fluids*, *30*, 3641–3643.

Haller, G., & Poje, A. C. (1998). Finite time transport in aperiodic flows. *Physica D*, *119*, 352–380.

Hammond, E. P., Bewley, T. R., & Moin, P. (1998). Observed mechanisms for turbulence attenuation and enhancement in opposition-controlled wall-bounded flows. *Physics of Fluids*, *10*(9), 2421–2423.

Jiménez, J. (1990). Transition to turbulence in two-dimensional Poiseuille flow. *Journal of Fluid Mechanics*, *218*, 265–297.

Jurdjevic, V., & Quinn, J. P. (1978). Controllability and stability. *Journal of Differential Equations*, *28*, 381–389.

Mezić, I., & Wiggins, S. (1999). A method for visualization of invariant sets of dynamical systems based on the ergodic partition. *Chaos*, *9*(1), 213–218.

Ottino, J. M. (1989). *The kinematics of mixing: Stretching, chaos, and transport*. Cambridge: Cambridge University Press.

Panton, R. L. (1996). *Incompressible flow* (2nd ed). New York: Wiley.

Poje, A. C., Haller, G., & Mezić, I. (1999). The geometry and statistics of mixing in aperiodic flows. *Physics of Fluids*, *11*(10).

Rom-Kedar, V., Leonard, A., & Wiggins, S. (1990). An analytical study of transport, mixing and chaos in an unsteady vortical flow. *Journal of Fluid Mechanics*, *214*, 347–394.

Rozhdestvensky, B. L., & Simakin, I. N. (1984). Secondary flows in a plane channel: Their relationship and comparison with turbulent flows. *Journal of Fluid Mechanics*, *147*, 261–289.

Ole Morten Aamo recieved his M.S. and Ph.D. degrees in Engineering Cybernetics from the Norwegian University of Science and Technology (NTNU) in 1992 and 2002, respectively. From 2002 to 2003 he was a post doctoral fellow at the Marine Technology Department at NTNU, and now holds a post doctoral position at the Engineering Cybernetics Department. Aamo is a co-author of the book Flow Control by Feedback (Springer-Verlag, 2002). His research interests include control of distributed parameter systems with special emphasis on fluid flows.

Miroslav Krstić is Professor and Vice Chair in the Department of Mechanical and Aerospace Egineering at University of California, San Diego. Prior to moving to UCSD, he was Assistant Professor in the Department of Mechanical Engineering and the Institute of Systems Research at University of Maryland (1995–97). He got his Ph.D. in Electrical Engineering from University of California at Santa Barbara, under Petar Kokotovic as his advisor, and received the UCSB Best Dissertation Award. Krstić is an IEEE Fellow and has received the National Science Foundation Career Award, the Office of Naval Research Young Investigator Award, the Presidential Early Career Award for Scientists and Engineers (PECASE), the George S. Axelby Outstanding Paper Award of IEEE Transactions on Automatic Control, and the O. Hugo Schuck Award for the best paper at American Control Conference. Krstić is a co-author of the books Nonlinear and Adaptive Control Design (Wiley, 1995), Stabilization of Nonlinear Uncertain Systems (Springer-Verlag, 1998), Flow Control by Feedback (Springer-Verlag, 2002), and Real Time Optimization by Extremum Seeking Control (Wiley, 2003). He is a co-author of two patents on control of aeroengine compressors and combustors. He has served as Associate Editor for the IEEE Transactions on Automatic Control, International Journal of Adaptive Control and Signal Processing, Systems and Control Letters, and Journal for Dynamics of Continuous, Discrete, and Impulsive Systems. Krstić is a Vice President for Technical Activities and a member of the Board of Governors of the IEEE Control Systems Society. His research interests include nonlinear, adaptive, robust, and stochastic control theory for finite dimensional and distributed parameter systems, and applications to fluid flows and fusion.

Prof. Thomas Bewley joined the Dynamic Systems and Control faculty at the University of California, San Diego in 1998, after completing his Ph.D. at the Center for Turbulence Research at Stanford University. The research interests of his Flow Control Lab at UCSD focus on the control, forecasting, and optimization of laminar, transitional, and turbulent flows. His work involves a blend of: large-scale simulations of chaotic fluid systems, modern linear and nonlinear control and optimization theory, characterization of controlled fluid systems with the inequalities available for Navier-Stokes systems, and the merging of these tools in order to provide new insights into important open problems in fluid mechanics. The work has relevance to applications such as drag reduction, mixing enhancement, noise mitigation, and weather prediction.